Research Article | Submit Manuscript

Turkish Journal of Material Sciences

Investigation of Deposition Parameters of Micro/Nanorod ZnO Thin Films with Ultrasonic Spray Pyrolysis Method

Eda Bingöl[1], Murat Tomakin[1,*]

[1]Recep Tayyip Erdoğan University, Faculty of Engineering, Department of Physics, Turkey

Published: 30.12.2017

Turk. J. Mater. Vol: 2 No: 2 Page: 31-37 (2017) ISSN: XXXX-YYYY

SLOI: http://www.sloi.org/sloi-name-of-this-article

*Correspondence E-mail: murattomakin@yahoo.com

ABSTRACT ZnO thin films were deposited on glass substrate by ultrasonic spray pyrolysis method in two steps: i) different substrate temperatures (between 300–500 °C, by 50 °C steps) and ii) different solution molarities (between 0.05 M – 0.25 M, step by 0.05 M). X-ray diffraction studies showed that the ZnO samples have hexagonal structures with preferred (002) directions. However, the preferred orientation decreased at substrate temperatures of 450 and 500 °C. Surface morphology of the ZnO samples completely changed from smooth and continuous form to hexagonal shaped microrods after 400 °C. ZnO nanorods with hexagonal shapes grew for 0.05 M. Composition ratio ([Zn]/[O]) of the samples decreased from 1.07 to 1.01 depending on substrate temperature. However, [Zn]/[O] ratio increased from 1.04 to 1.09 with increasing molarity. A sharp ultraviolet luminescence was observed at ~380 nm for higher substrate temperatures and molarity values. Band gap values decreased from 3.27 eV to 3.19 eV by increasing substrate temperature. Solution molarity did not significantly affect band gap values (3.20–3.22 eV) of the samples. Lower resistivity (1.56×10^{3} Ω-cm) and higher carrier concentration values (1.27×10^{15} cm^{-3}) were obtained at substrate temperatures of 400 °C and solution molarity of 0.15 M.

Keywords: ZnO; Micro/Nanorod; Spray Pyrolysis; Thin Film.

Cite this article: E. Bingöl, M. Tomakin. Investigation of Deposition Parameters of Micro/Nanorod ZnO Thin Films with Ultrasonic Spray Pyrolysis Method. 2(2) (2017) 31-37.

1. INTRODUCTION

Considering recent studies on electronic devices, it is understood that micro- and nano-structured semiconductor materials are becoming very important. Especially, nanomaterials attract more interest than bulk materials due to quantum-size effects [1]. One of the most commonly used materials in technological researches based on micro- and nano-structured materials is zinc oxide (ZnO). ZnO has an important place among II-VI semiconductor materials due to wide and direct band gap of about 3.37 eV, higher exciton binding energy (60 meV) at room temperature, low cost and environmental friendly. Therefore, ZnO has a wide range of applications such as solar cells, light emitting diodes, optoelectronic devices, gas sensors and biosensor [2]. Also, ZnO is used in pharmaceutics, cosmetics, food science and agriculture [3]. Control of the dimensions and morphology of materials has attracted the interest of researchers to design functional devices due to the optical and electronic properties of nanometer and micrometer-size materials [4]. Depending on the production method, ZnO can be obtained in different morphologies such as microsphere [5], microcomb [6], nanorod [7], nanowire [8] and nanosheet [9]. Micro- and nano-rod shaped ZnO thin films are attracting great interest for device applications due to their different morphology, large surface area and high aspect ratio. So, obtaining good-orientation ZnO rods with high optical quality, uniform thickness and length distribution is important for the preparation of different devices.

Micro- and nano-structured semiconductor thin film samples can be prepared by spray pyrolysis method

which is one of the simple and inexpensive methods. The key parameters in the spraying method are the atomization form, the transport of the sprayed material (carrier gas, pressure, distance), the substrate temperature, the substrate material and most importantly the chemical composition of the solution. Nowadays, spray by ultrasonic nebulizer has come into one of the most powerful methods for preparation of nanostructured materials [10]. Previously our research group prepared ZnO microrods by ultrasonic spray pyrolysis method and investigated the correlation between structural and optical properties of the ZnO thin films and substrates. In this study, ZnO thin films were deposited on glass substrates by ultrasonic spray pyrolysis (USP) method to investigate the effects of substrate temperature and solution molarity on structural, optical and electrical properties of the ZnO thin films. The aim of this study is to obtain good-orientation ZnO micro/nanorods with high optical quality, uniform thickness, and length distribution.

2. EXPERIMENTAL

ZnO thin films were grown on glass substrates by ultrasonic spray pyrolysis in air atmosphere. Experimental procedures were performed in two steps: i) different substrate temperatures and ii) different solution molarities. In first step, ZnO thin films were prepared at different substrate temperatures of 300 °C, 350 °C, 400 °C, 450 °C and 500 °C. Glass substrates were cleaned ultrasonically with acetone, ethanol, and deionized water, respectively and then the substrates were dried by air flow. The initial solution was prepared from zinc chloride ($ZnCl_2$) at 0.15 M concentration in deionized water. The precursor solution was nebulized by an ultrasonic generator with approximately 1.7 MHz. The growth time of the all thin films was 50 min. The solution spray rate and carrier gas (air) flow rate were 2 ml/min and 8 l/min, respectively. The substrate–nozzle distance was 10 cm. During growth, the substrates were rotated at 3.5 rpm to produce uniform and homogenous films. In second step, ZnO samples were prepared by using different solution molarities (0.05 M, 0.10 M, 0.15 M, 0.20 M and 0.25 M) at the same substrate temperature of 400 °C. The other parameters were the same with first step. The crystal structure of CdS thin films was examined by X-ray diffraction (XRD) using Rigaku Smartlab with CuK_α radiation (λ = 1.5408 Å) over the range 2θ = 30–60° at room temperature. Morphological information was obtained by JEOL JSM 6610 scanning electron microscope (SEM). Elemental analysis was studied by using Oxford Instruments Inca X-act energy dispersive X-ray spectroscopy (EDS) attached to the SEM. Room temperature photoluminescence (RTPL) spectra were measured using SpectraMax M5 spectrophotometer with a xenon flash lamp as light source operating at 280 nm with an output power of 150 W. Optical transmittance measurements were performed at room temperature between 300 – 1000 nm by SpectraMax M5 spectrophotometer. The hot probe method and Hall Effect measurements (in dark) were used to find carrier type and carrier density of the ZnO thin films at room temperature. The all ZnO samples had n-type conductivity. Resistivity values of the ZnO thin films were obtained by Van der Pauw method in dark at room temperature.

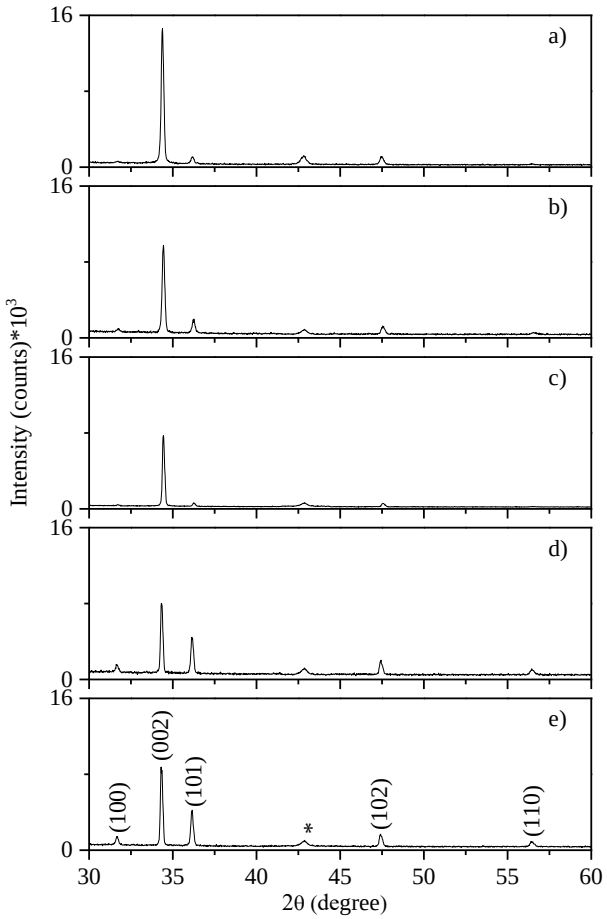


Figure 1. *XRD patterns of the ZnO thin films prepared at a) 300 ℃, b) 350 ℃, c) 400 ℃, d) 450 ℃ and e) 500 ℃.*

3. RESULTS

XRD results of the ZnO samples prepared at different substrates temperatures were shown Fig. 1. The ZnO thin films had hexagonal structure with the (002) preferred orientation plane. The peak intensity of the (002) plane decreased with increasing substrate temperature. Up to 400 °C substrate temperature, the peak intensity of the (002) plane was not changed significantly. However, preferred orientation decreased for 450 °C and 500 °C substrate temperatures due to the formation of relatively highly intensive (100), (101), (102) and (110) peaks which are planes of hexagonal structure [11]. Decreasing of the peak intensity and evolution of the preferred orientation for higher substrate temperatures were attributed to changing surface morphology of the samples from smooth and continuous form to microrods (Fig.3.). Fig. 2 shows XRD results of the ZnO thin films prepared at different molarities. As can be seen from this figure, hexagonal crystal structure with the (002) preferred orientation was obtained for the ZnO thin films. Intensity of the (002) plane related to the and preferred orientation increased with increasing molarity. This result was attributed to increasing grain size (Fig. 4.) and film thickness (Table 1.) with molarity [12,13]. Above 0.15 M, the peak intensity of the (002) plane related to the preferred orientation was approximately the same. A

small diffraction peak about 43° (*) was observed in

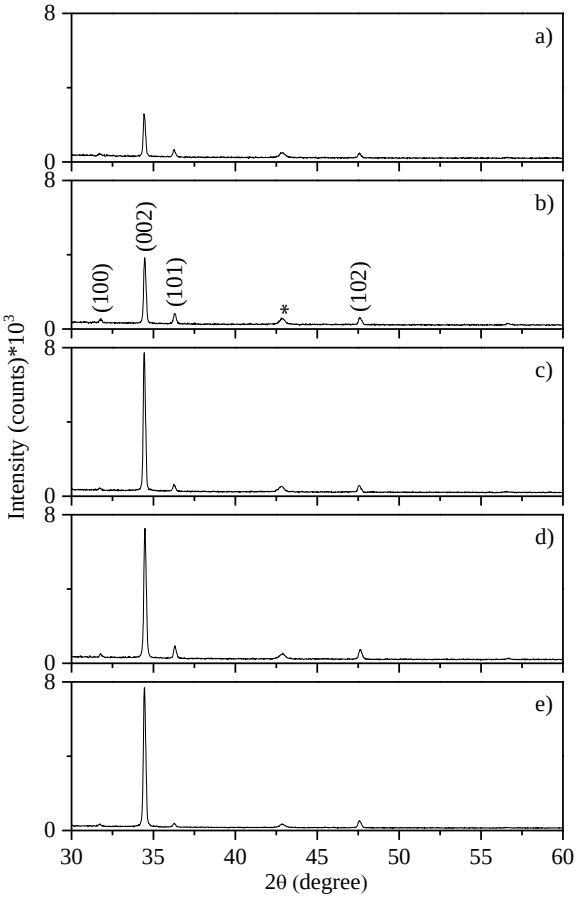


Figure 2. *XRD patterns of the ZnO thin films prepared by using a) 0.05 M, b) 0.10 M, c) 0.15 M, d) 0.20 M and e) 0.25 M.*

XRD patterns of the all thin films. This peak can be explained with (200) plane of the ZnO cubic phase (PDF Card No.: 01-077-9353). Also, the orthorhombic Zn_2SiO_4 (zinc silicate) phase has (004) diffraction peak about 43° (PDF Card No.: 00-024-1469). Zn_2SiO_4 phase can be formed due to relatively high deposition temperature of the ZnO thin films. Similar results were found by another researcher for the ZnO samples [1,14]. The lattice parameters *a* and *c* were calculated from the positions of the XRD peaks of the hexagonal phase. The calculated lattices parameters were listed Table 1. The lattice parameters of the ZnO samples are comparable with the lattice parameters of bulk ZnO (a = 3.249 Å and c = 5.206 Å). However, *a* and *c* values of the ZnO thin films prepared at higher substrate temperatures of 450 and 500 °C substrate were relatively higher than that of the bulk ZnO.

The cross-sectional SEM micrographs of the films were applied to determine film thickness (Table 1). Thickness of the ZnO samples increased from 0.75 μm to 1.12 μm with increasing substrate temperature. Above 400 °C, thickness decreased from 1.12 μm to 0.95 μm and then remained almost the same. Similar thickness behavior was found for the ZnO thin films prepared with different molarities. Firstly thickness increased from 0.51 μm to 1.12 μm with molarity. For high molarity values thickness was constant about 1.03 μm. The surface morphologies of the ZnO thin films were investigated by SEM and the results were shown in Fig. 3 and Fig. 4. As seen in Fig. 3, substrate temperature had a significant effect on the surface morphology of the samples. The sample prepared at 300 °C had smooth and continuous surface morphology. For applied substrate temperature of 350 °C, some rod like grains are formed. Above 400 °C, surface morphology of the ZnO samples completely changed to hexagonal shaped microrods. However, the surface of the ZnO microrods had some voids. Some researcher found similar hexagonal shaped microrod structures for the ZnO thin films prepared with spray pyrolysis method [15–17]. The width of microrods increased from 0.4 μm to 1 μm, although the height of microrods was almost the same anddidnot affected by increased substrate temperature. So, width/height ratio of ZnO microrods for high substrate temperatures increased toward ~1. Also, while microrods in the ZnO sample prepared at 400 °C had highly *c*-axis orientation on substrate surface, the *c*-axis orientation on substrate surface of microrods for the ZnO samples prepared at 450 °C and 500 °C decreased. This orientation differences are consistent with XRD measurements (Fig. 2.). Fig. 4 shows SEM images of the ZnO samples prepared with different molarities. As can be seen from this figure, the ZnO sample for 0.05 M grew as hexagonal shaped nanorod (width/height ~1/5). Rod width increased from 0.1 μm to 0.7 μm with molarity and grain structure of the samples changed from nanorods to microrods for high molarities. The all ZnO samples prepared with different molarities had *c*-axis orientation on substrate surface. The composition ratio of the films was determined by EDS analysis. The atomic percent (at.%) of Zn and O in the films are listed in Table 1. Composition ratio ([Zn]/[O]) of the samples decreased from 1.07 to 1.01 depending on substrate temperature. The [Zn]/[O] ratio for the samples prepared with different molarities increased from 1.04 to 1.09 by increasing molarity. As a result, the samples prepared at high substrate temperature were more stoichiometric than the other samples.

Room temperature photoluminescence behavior (RTPL) was investigated for determining of the optical properties and structural defects. Fig. 5 a) shows RTPL spectra of the ZnO samples prepared at different substrate temperatures. Main luminescence peak of the ZnO samples was near band edge UV emission, which observed at approximately 380 nm. The origin of near band edge UV emission is due to the free exciton recombination [18]. The UV luminescence formed lower intensity for the ZnO samples prepared at 300 °C.

Table 1. *The lattice parameters, thickness and atomic concentrations of the ZnO samples.*

T_S (°C)	a (Å)	c (Å)	t (μm)	[Zn] (at.%)	[O] (at.%)	[Zn]/[O]
300	3.260	5.219	0.75	51.7	48.3	1.07
350	3.258	5.213	0.70	51.4	48.6	1.06
400	3.256	5.213	1.12	51.2	48.8	1.05
450	3.264	5.229	0.95	50.4	49.6	1.02
500	3.265	5.231	0.96	50.3	49.7	1.01
Molarity (M)						
0.05	3.255	5.213	0.51	51.0	49.0	1.04
0.10	3.251	5.209	0.62	50.7	49.3	1.03
0.15	3.256	5.213	1.12	51.2	48.8	1.05
0.20	3.252	5.207	1.03	51.5	48.5	1.06
0.25	3.254	5.211	1.02	52.1	47.9	1.09

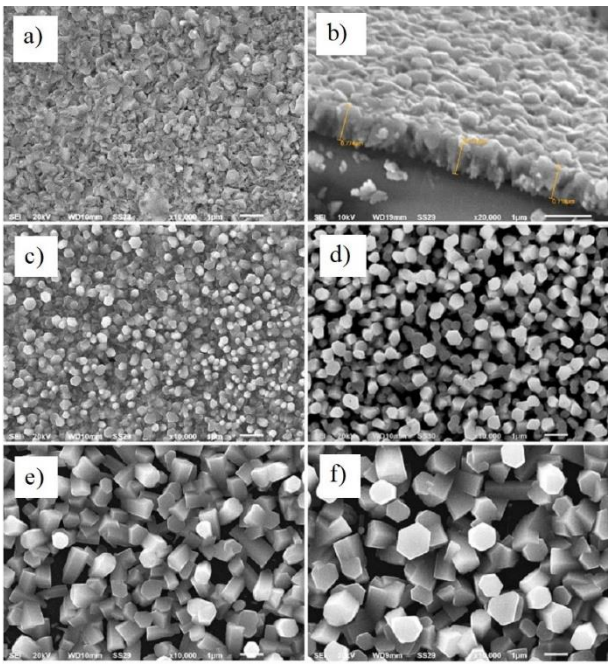


Figure 3. *SEM images of the ZnO thin films for a) 300 ℃, b) cross-section image for 300 ℃, c) 350 ℃, d) 400 ℃, e) 450 ℃ and f) 500 ℃*

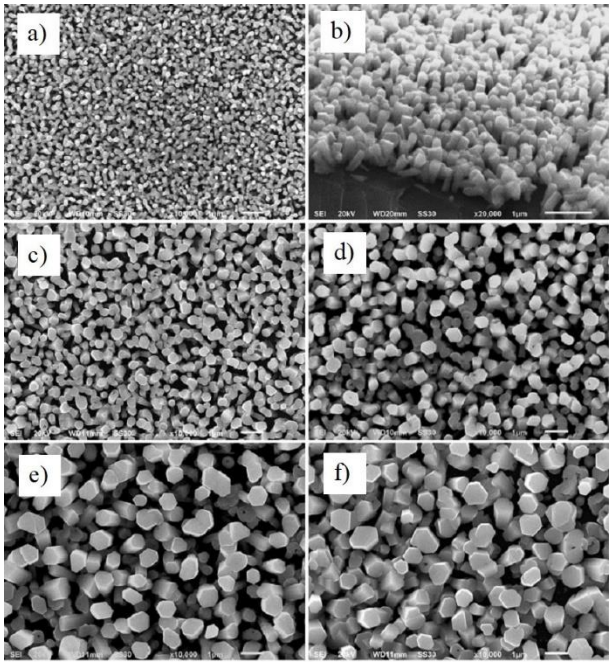


Figure 4. *SEM images of the ZnO thin films for a) 0.05 M, b) cross-section image for 0.05 M, c) 0.10 M, d) 0.15 M, e) 0.20 M and f) 0.25 M.*

Intensity of this UV peak increased with substrate temperature. Sharp and predominant UV luminescence was observed for the ZnO thin films prepared at 400 °C. However, UV peak intensity decreased for the ZnO thin films prepared at 450 °C and 500 °C. We found that although the ZnO thin films prepared at 400 °C, 450 °C and 500 °C had lower peak intensity in XRD pattern, they had higher UV intensity, which is reverse in the expected situation. This result can be explained with increasing of thickness and improving of stoichiometry for the ZnO thin films prepared at 400 °C, 450 °C and 500 °C. The reason of decreasing of UV peak intensity for higher substrate temperatures of 450 and 500 °C is deteriorating of preferred orientation and so crystal quality [19]. UV peak position slightly shifted from 377 nm to 380 nm as substrate temperature increased from 300 °C to 400 °C, which shows that the band gap decreased from 3.29 eV to 3.27 eV. This result is consistent with partially the band gap values obtained from optical transmittance. After 400 °C, UV peak position was not changed. RTPL spectra of the ZnO samples prepared with different molarities were shown in Fig. 5 b). As can be seen this figure, UV luminescence intensity increased with molarity. However, the UV peak intensity was approximately constant for 0.15 M, 0.20 M and 0.25 M.

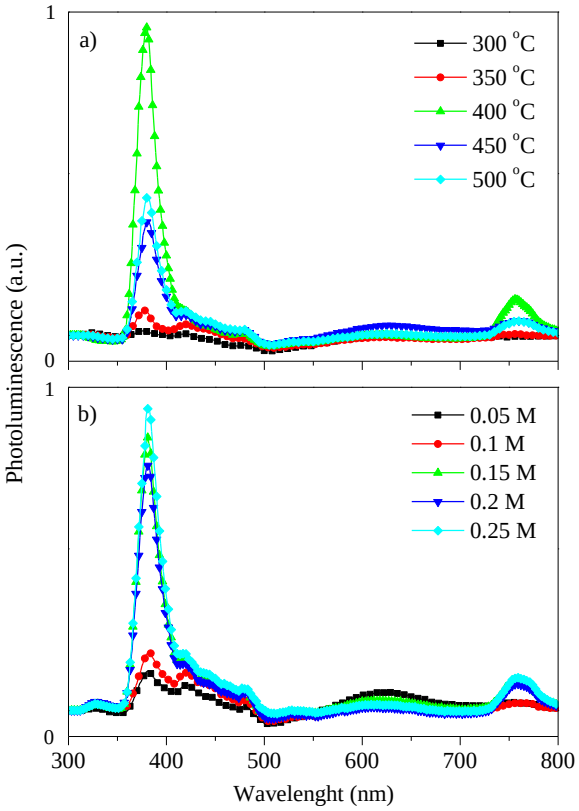


Figure 5. *Room temperature photoluminescence spectra of the ZnO thin films for a) different substrate temperatures and b) different molarities.*

These results can be attributed from that the ZnO thin films prepared with 0.15 M, 0.20 M and 0.25 M had higher XRD intensity, higher thickness and larger grain size. Solution molarity did not change UV peak position at 380 nm, which are not agreement with the variations in the band gap value determined by the optical transmittance. The reason of this difference is that the Tauc relation assumes free carrier behavior with no electron–hole interactions, whereas for ZnO the large excitonic binding energy of 60 meV means that significant electron–hole correlation is present even at room temperature [20]. As seen from Fig. 5 a and b, the ZnO samples with microrod structure had predominant UV luminescence. The peak at 756 nm, which was not observed for 300 °C substrate temperature, is related to second-order properties of the UV peak [21]. Defects

peaks were observed between 400–500 nm and 500–700 nm for RTPL spectra of the ZnO samples. The peaks between 400–500 nm can be formed due to interstitial zinc atoms at 420 nm, transitions of interstitial Zn levels to vacancy Zn levels at 440 nm and transitions of interstitial O levels to vacancy O levels at 480 nm [15,22]. The emission region between 500 – 700 nm can be formed due to vacancy Zn, interstitial Zn, vacancy O, interstitial O and anti-sites defects at 530 nm[21,23] and O and Zn anti-sites around 625 nm [24]. Defect peak at 530 nm was observed only in the ZnO samples with microrod structure. As a result, the origin of the defect peaks at range 400–700 nm is controversial because of complicated extrinsic and intrinsic defects in ZnO [25].

Optical transmittance measurement of the ZnO thin films prepared at different substrate temperatures were shown in Fig. 6 a. The high optical transmittance was obtained for 300 °C. As increasing substrate temperature, transmittance of the samples decreased dramatically. After 400 °C, transmittance was not changed significantly. It is known that optical transmittance in growing rod morphology of sprayed ZnO samples is very low compared to their thin film counterparts [26]. Also, the ZnO thin films prepared at 300 °C and 350 °C had sharp band edge transition than other samples, which is an indication of good crystallinity. This result verifies XRD measurement in Fig. 1. Fig. 6 b shows effect of molarity on optical transmittance. It can be seen from this figure that optical transmittance decreased with solution molarity. However, optical transmittance of ZnO microrods prepared with 0.15 M, 0.20 M and 0.25 M was approximately the same. Sharpness of the band edge transition of ZnO nanorods prepared with 0.05 M was lower than that of other samples. Also, optical transmittance of ZnO nanorods exhibited a constantly increasing behavior with wavelength. These behaviors obtained for 0.05 M are observed generally in nanostructured materials due to the presence of high light scattering centers or other defects [27]. The band gap energy E_g of the ZnO thin films was determined using Tauc relation $\alpha h\nu = A(h\nu - E_g)^{1/2}$, where α is the absorption coefficient, E_g is the optical band gap and A is a constant. Obtained band gap values of the samples were listed in Table 2. The band gap of ZnO single crystal is about 3.37 eV which is higher than that of the band gap values in Table 2. The observed lower band gap value could be originated from the native point defects such as oxygen vacancies and zinc interstitials [15]. The band gap of the ZnO samples prepared different substrate temperatures decreased from 3.27 eV to 3.19 eV as increasing of substrate temperature. The decreasing in the band gap can be due to the influence of various factors such as grain size, carrier concentration, deviation from the stoichiometry and lattice strain[28–30]. The possible mechanism of the decreasing in the band gap could be ascribed to increase in thickness and grain size and to improve in stoichiometry. As solution molarity increased from 0.05 M to 0.15 M, the band gap increased from 3.20 eV to 3.22 eV, and then remained constant at 3.22 eV for high molarities. A similar behavior for the band gap was found by Mariappan et al [31]. In the study of Mariappan et al, the band gap of the ZnO samples prepared with nebulizer spray pyrolysis method increased from 3.12 eV to 3.20 eV with increasing molarity (from 0.05 M to 0.15 M).

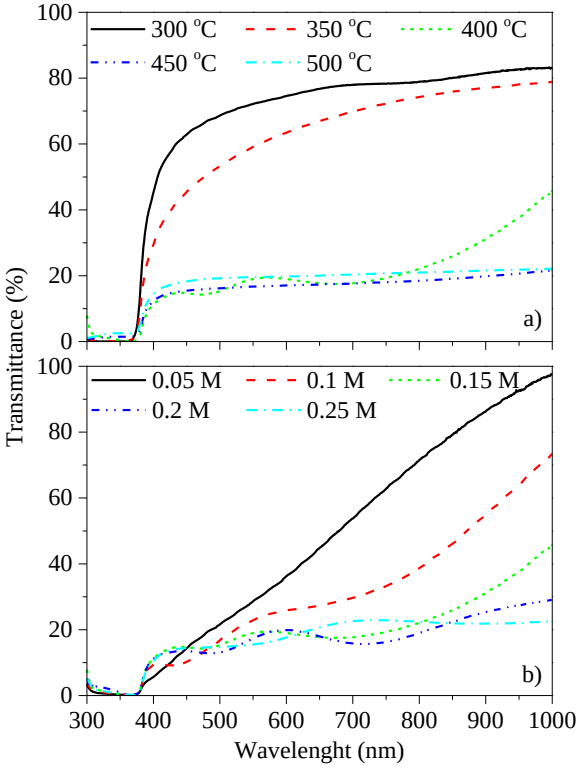


Figure 6. *Optical transmittance spectra of the ZnO thin films for a) different substrate temperatures and b) different molarities.*

The resistivity and the carrier concentration of the all ZnO films were listed in Table 2. It is known that interstitial zinc I_{Zn} and oxygen vacancies V_O are donor-type defects and they increase the carrier concentration of the ZnO samples. Better stoichiometry decreases these defects and hence carrier concentration decreases [32]. Also, increasing of thickness and grain size decreases surface effect, grain boundary scattering and trapping centers at grain boundaries and so carrier concentration, electron mobility and electrical conductivity increase [33]. Therefore, one should consider the different competing processes in evaluating the measured resistivity and carrier concentration values. The resistivity values of the ZnO samples prepared at different substrate temperatures decreased slightly from 5.63×10^3 Ω-cm to 1.56×10^3 Ω-cm as the substrate temperature increased from 300 °C to 400 °C. After 400 °C, resistivity increased to 1.05×10^4 Ω-cm. The behavior of the carrier concentration with substrate temperature is compatible with the resistivity behavior, so that the carrier concentration increased from 4.12×10^{14} cm^{-3} to 1.27×10^{15} cm^{-3} as the substrate temperature increased from 300 °C to 400 °C, and then decreased 7.10×10^{13} cm^{-3} for 500 °C. The decreasing in the resistivity (or increasing of the carrier concentration) can be explained with increasing of the thickness and grain size as the substrate temperature increased from 300 °C to 400 °C. For substrate temperatures of 450 and 500 °C the increasing in the resistivity (or decreasing of the carrier concentration) due to increasing of voids density on

surface of the ZnO thin films that it becomes more difficult for carriers to travel from one grain to neighboring grains [34]. Also, the decreasing of orientation of the microrods for higher substrate temperatures of 450 and 500 °C can be increased the resistivity due to the fact that the entangled microrods prevent direct path for efficient electron transfer [35]. The resistivity values for the ZnO samples prepared with different molarities decreased from 1.13×10^4 Ω-cm to 1.56×10^3 Ω-cm as the molarity increased from 0.05 M to 0.15 M. However, the resistivity increased slightly to 2.38×10^3 Ω-cm after 0.15 M. The carrier concentration of the ZnO samples prepared with different molarities increased from 1.42×10^{13} cm^{-3} to 1.27×10^{15} cm^{-3} with increasing molarity. After 0.15 M, the carrier concentration decreased to 7.12×10^{14} cm^{-3}. This behavior of the carrier concentration verifies to the resistivity behavior with molarity. High resistivity and low carrier concentration values for low molarities can be explained with the decrease in the grain size and so increasing the grain boundaries. The resistivity and the carrier concentration values of our samples were between 10^3–10^4 Ω-cm and 10^{13}–10^{15} cm^{-3}, respectively. These values are agreement with the results found by Manoharan et al [32]. However, Chen et al were found the resistivity and the carrier concentration of the ZnO sample in order of 10^{-1} Ω-cm and 10^{20} cm^{-3}, respectively [36]. As a result, it can be said that the best values for the resistivity and the carrier concentration were obtained in the sample prepared at 400 °C with 0.15 M, and high substrate temperature and low molarity deteriorated significantly electrical parameters.

Table 2. *Band gap, resistivity and carrier concentration values of the ZnO thin films*

T_S (°C)	E_g (eV)	ρ (Ω-cm)	n (cm^{-3})
300	3.27	5.63×10^3	4.12×10^{14}
350	3.25	4.17×10^3	4.74×10^{14}
400	3.22	1.56×10^3	1.27×10^{15}
450	3.20	7.39×10^3	3.81×10^{14}
500	3.19	1.05×10^4	7.10×10^{13}
Molarity (M)			
0.05	3.20	1.13×10^4	1.42×10^{13}
0.10	3.21	5.35×10^3	5.47×10^{14}
0.15	3.22	1.56×10^3	1.27×10^{15}
0.20	3.22	2.71×10^3	6.35×10^{14}
0.25	3.22	2.38×10^3	7.12×10^{14}

4. CONCLUSION

Structural, optical and electrical properties of the ZnO thin films grown by ultrasonic spray pyrolysis at different substrate temperatures and molarities were investigated. X-ray diffraction studies showed that the (002) preferred direction by hexagonal ZnO samples increased with an increase in the molarity. However, increasing substrate temperature affected the preferential orientation negatively. The lattice parameters of the ZnO samples were comparable with the lattice parameters of bulk ZnO except for the ZnO thin films prepared at higher substrate temperatures of 450 and 500 °C. Surface morphology changed from continuous form to a microrods with hexagonal shape for higher substrate temperature (> 350 °C). For the sample prepared with 0.05 M molarity, surface morphology of the ZnO sample was hexagonal shaped nanorod. The thickness of the ZnO samples increased from 0.70 μm and 0.51 μm to ~1 μm with substrate temperature and molarity, respectively. The [Zn]/[O] composition ratio of the ZnO samples improved by increasing substrate temperature. Photoluminescence measurements indicated the existence of three emission bands in the spectra: a sharp ultraviolet luminescence at ~380 nm, and two broad visible defect related emissions between 400–500 nm and between 500–700 nm. By increasing substrate temperature, transmittance of the samples decreased dramatically from 80 to 20 %.

Acknowledgement

This work was supported by the research fund of Recep Tayyip Erdoğan University, Rize, Turkey, under Contract No. 2014.102.01.02.

References

[1] I. Polat, S. Yılmaz, I. Altın, E. Bacaksız, M. Sokmen, The influence of Cu-doping on structural, optical and photocatalytic properties of ZnO nanorods, Mater. Chem. Phys. 148 (2014) 528–532.

[2] M. Salem, S. Akir, T. Ghrib, K. Daoudi, M. Gaidi, Fe-doping effect on the photoelectrochemical properties enhancement of ZnO films, J. Alloys Compd. 685 (2016) 107–113.

[3] D. Thomas, J. Abraham, S.C. Vattappalam, S. Augustine, T.D. Thomas, Antibacterial activity of pure and cadmium doped ZnO thin film, Indo Am. J. Pharm. Res. 4 (2014) 1612–1616.

[4] D.J. Milliron, S.M. Hughes, Y. Cui, L. Manna, J. Li, L.-W. Wang, A.P. Alivisatos, Colloidal nanocrystal heterostructures with linear and branched topology, Nature. 430 (2004) 190–195.

[5] X. Wang, X. Xie, X. Song, J. Tian, S. Ma, H. Cui, Fabrication of Au decorated porous ZnO microspheres with enhanced gas sensing properties, Powder Technol. 315 (2017) 379–384.

[6] X. Huang, J. Xia, C. Luan, M. Sun, X. Wang, G.-W. She, C.-S. Lee, X.-M. Meng, The structural and optical properties of a single ZnO comb and an individual nail-like tooth, CRYSTENGCOMM. 15 (2013) 10604–10610.

[7] B.-C. Lina, C.-S. Kub, H.-Y. Lee, A.T. Wua, Epitaxial growth of ZnO nanorod arrays via a self-assembled microspheres lithography, Appl. Surf. Sci. 414 (2017) 212–217.

[8] Z.-W. Wu, S.-L. Tyan, C.-R. Lee, T.-S. Mo, Bidirectional growth of ZnO nanowires with high optical properties directly on Zn foil, Thin Solid Films. 621 (2017) 102–107.

[9] E. Modaresinezhad, S. Darbari, Realization of a room-temperature/self-powered humidity sensor, based on ZnO nanosheets, Sensors Actuators B Chem. 237 (2016) 358–366.

[10] J.H. Bang, K.S. Suslick, Applications of Ultrasound to the Synthesis of Nanostructured Materials, Adv. Mater. 22 (2010) 1039–1059.

[11] M. Tomakin, Z. Onuk, N. Rujisamphan, S.I. Shah, Role of the radio frequency magnetron sputtered seed layer properties on ultrasonic spray pyrolyzed ZnO thin films, Thin Solid Films. 642 (2017) 163–168.

[12] M.R. Prasad, M. Haris, M. Sridharan, Structural, optical and ammonia sensing properties of nanostructured ZnO thin films deposited by spray pyrolysis technique, J. Mater. Sci. Mater. Electron. 28 (2017) 11367–11373.

[13] U. Chaitra, D. Kekuda, K.M. Rao, Dependence of solution molarity on structural, optical and electrical properties of spin coated ZnO thin films, J. Mater. Sci. Mater. Electron. 27 (2016) 7614–7621.

[14] S. Yılmaz, E. Bacaksız, İ. Polat, Y. Atasoy, Fabrication and structural, electrical characterization of i-ZnO/n-ZnO nanorod homojunctions, Curr. Appl. Phys. 12 (2012) 1326–1333.

[15] M. Tomakin, Structural and optical properties of ZnO and Al-doped ZnO microrods obtained by spray pyrolysis method using different solvents, Superlattices Microstruct. 51 (2012) 372–380.

[16] U. Alver, T. Kılınc, E. Bacaksız, S. Nezir, Temperature dependence of ZnO rods produced by ultrasonic spray pyrolysis method, Mater. Chem. Phys. 106 (2007) 227–230.

[17] S.J. Ikhmayies, Synthesis of ZnO Microrods by the Spray Pyrolysis Technique, J. Electron. Mater. 45 (2016) 3964–3969.

[18] H. Y.-M., L. S.-Y., Z. S.-M., Y. R.-J., Z. G.-Y., L. N, Structural. optical. and magnetic studies of manganese-doped zinc oxide hierarchical microspheres by self-assembly of nanoparticles, Nanoscale Res. Lett. 7 (2012) 111–113.

[19] Y. Luo, H. Liu, High optical quality ZnO films grown on graphite substrate for transferable optoelectronics devices by ultrasonic spray pyrolysis, Mater. Res. Bull. 47 (2012) 2685–2688.

[20] S. Yılmaz, M. Parlak, Ş. Özcan, M. Altunbaş, E. McGlynn, E. Bacaksız, Structural, optical and magnetic properties of Cr doped ZnO microrods prepared by spray pyrolysis method, Appl. Surf. Sci. 257 (2011) 9293–9298.

[21] F. Yi, Y. Huang, Z. Zhang, Q. Zhang, Y. Zhang, Photoluminescence and highly selective photoresponse of ZnO nanorod arrays, Opt. Mater. (Amst). 35 (2013) 1532–1537.

[22] G. Srinet, R. Kumar, V. Sajal, Effects of aluminium doping on structural and photoluminescence properties of ZnO nanoparticles, Ceram. Int. 40 (2014) 4025–4031.

[23] G. Srinet, P. Varshneya, R. Kumar, V. Sajal, P.K. Kulriya, M. Knobel, S.K. Sharma, Structural, optical and magnetic properties of Zn1-xCoxO prepared by the sol–gel route, Ceram. Int. 39 (2013) 6077–6085.

[24] R.S. Zeferino, M.B. Flores, U. Pal, Photoluminescence and Raman scattering in Ag-doped ZnO nanoparticles, J. Appl. Phys. 109 (2011) 14308.

[25] R.C. Pawar, H. Kim, C.S. Lee, Defect-controlled growth of ZnO nanostructures using its different zinc precursors and their application for effective photodegradation, Curr. Appl. Phys. 14 (2014) 621–629.

[26] S. Yılmaz, İ. Polat, Y. Atasoy, E. Bacaksız, Structural, morphological, optical and electrical evolution of spray deposited ZnO rods co-doped with indium and sulphur atoms, J. Mater. Sci. Mater. Electron. 25 (2014) 1810–1816.

[27] A.C. Aragonès, A. Palacios-Padrós, F. Caballero-Briones, F. Sanz, Study and improvement of aluminium doped ZnO thin films: Limits and advantages, Electrochim. Acta. 109 (2013) 117–124.

[28] V.D. Novruzov, E.F. Keskenler, M. Tomakin, S. Kahraman, O. Gorur, Effects of ultraviolet light on B-doped CdS thin films prepared by spray pyrolysis method using perfume atomizer, Appl. Surf. Sci. 280 (2013) 318– 324.

[29] M.A. Redwan, L.I. Soliman, E.H. Aly, A.A. El-Shazely, H.A. Zayed, Study of electrical and optical properties of Cd1 − xZnxS thin films, J. Mater. Sci. 38 (2003) 3449–3454.

[30] H. Chavez, M. Jordan, J.C. McClure, G. Lush, V.P. Singh, Physical and electrical characterization of CdS films deposited by vacuum evaporation, solution growth and spray pyrolysis, J. Mater. Sci. Mater. Electron. 8 (1997) 151–154.

[31] R. Mariappan, V. Ponnuswamy, M. Ragavendar, Influence of molar concentration on the physical properties of nebulizer-sprayed ZnO thin films for ammonia gas sensor, Mater. Sci. Semicond. Process. 16 (2013) 1328–1335.

[32] C. Manoharan, S. Dhanapandian, A. Arunachalam, M. Bououdina, Physical properties of spray pyrolysized nano flower ZnO thin films, J. Alloys Compd. 685 (2016) 395–401.

[33] M. Jlassi, I. Sta, M. Hajji, H. Ezzaouia, Effect of nickel doping on physical properties of zinc oxide thin films prepared by the spray pyrolysis method, Appl. Surf. Sci. 301 (2014) 216–224.

[34] A. Zhong, J. Tana, H. Huang, S. Chen, M. Wang, S. Xu, Thickness effect on the evolution of morphology and optical properties of ZnO films, Appl. Surf. Sci. 257 (2011) 4051–4055.

[35] K.V. Gurav, U.M. Patil, S.M. Pawar, J.H. Kim, C.D. Lokhande, Controlled crystallite orientation in ZnO nanorods prepared by chemical bath deposition: Effect of H2O2, J. Alloys Compd. 509 (2011) 7723– 7728.

[36] K. Ravichandran, N. Dineshbabu, T. Arun, C. Ravidhas, S. Valanarasu, Effect of fluorine (an anionic dopant) on transparent conducting properties of Sb (a cationic) doped ZnO thin films deposited using a simplified spray technique, Mater. Res. Bull. 83 (2016) 442–452.